Bioorganic & Medicinal Chemistry Letters 21 (2011) 1832–1837

Contents lists available at ScienceDirect

Bioorganic & Medicinal Chemistry Letters

journal homepage: www.elsevier.com/locate/bmcl

Maintaining potent HTLV-I protease inhibition without the P_3-cap moiety in small tetrapeptidic inhibitors

Jeffrey-Tri Nguyen, Keiko Kato, Henri-Obadja Kumada, Koushi Hidaka, Tooru Kimura, Yoshiaki Kiso *

Department of Medicinal Chemistry, Center for Frontier Research in Medicinal Science, Kyoto Pharmaceutical University, Yamashina-ku, Kyoto 607-8412, Japan

ARTICLE INFO

Article history:
Received 15 December 2010
Revised 11 January 2011
Accepted 12 January 2011
Available online 15 January 2011

Keywords:
Human T cell lymphotropic virus
Adult T cell leukemia
Aspartic protease
Inhibitor
Retrovirus

ABSTRACT

The human T cell lymphotropic/leukemia virus type 1 (HTLV-I) causes adult T cell lymphoma/leukemia. The virus is also responsible for chronic progressive myelopathy and several inflammatory diseases. To stop the manufacturing of new viral components, in our previous reports, we derived small tetrapeptidic HTLV-I protease inhibitors with an important amide-capping moiety at the P_3 residue. In the current study, we removed the P_3-cap moiety and, with great difficulty, optimized the P_3 residue for HTLV-I protease inhibition potency. We discovered a very potent and small tetrapeptidic HTLV-I protease inhibitor (KNI-10774a, IC_{50} = 13 nM).

The human T cell lymphotropic/leukemia virus type 1 (HTLV-I) is the only human retrovirus known to cause cancer. It is estimated that 20–30 million people are infected with HTLV-I worldwide,[1] with endemic foci in southern Japan, western Africa, Central and South America,[2] transmitted by close contact with infected T lymphocytes via breast-feeding,[3] sexual intercourse, and parenteral exposure to blood.[4] Infection with HTLV-I is lifelong with an asymptomatic carrier state lasting 20–50 years[5] that progresses to aggressive conditions: either adult T cell lymphoma/leukemia (ATL)[6] or HTLV-I associated myelopathy/tropical spastic paraparesis (HAM/TSP).[7] The retrovirus in ATL patients is resistant to conventional chemotherapy,[8] and there is presently no cure for HTLV-I infection. Current treatment regimens for HIV-1 infection in highly active anti-retroviral therapy (HAART) include HIV-1 protease inhibitors. HTLV-I protease grossly resembles HIV-1 protease with both being homodimers that form in a pincer shape with a flap region and a central active site region where a trapped precursor protein is cleaved into peptides.[9] Inhibiting the protease with an antagonist prevents the processing of precursor proteins and consequently stops viral replication. Several commercial HIV-1 protease inhibitors such as ritonavir,[10] amprenavir, saquinavir, indinavir, and nelfinavir,[11] were shown ineffective against HTLV-I protease, most likely because HTLV-I protease is larger than HIV-1 protease (125 vs 99 amino acids per chain), and shares only an overall 28% sequence identity and 45% sequence identity at the active site.[9] Based on the matrix–capsid cleaving region of precursor proteins, one of our initial HTLV-I protease inhibitor design (**1**) had a hydroxymethylcarbonyl isostere as a central inhibitory unit ('warhead') against the protease's two catalytic aspartic acid residues (Fig. 1).[10] After several structure-based drug design optimization to improve potency while decreasing molecular size from octapeptidic inhibitors, we derived an isoleucine laden inhibitor (**2**).[12] Further optimization and removal of natural amino acids led to a small yet very potent inhibitor against HTLV-I protease, KNI-10635 (**3**), comprising of four amino acid residues with two end-capping moieties (Table 1, Fig. 2).[13–15] Herein, we describe our arduous attempt to remove the N-terminal cap moiety which significantly contributes to inhibitory potency.

HTLV-I protease was shown to display a high degree of specificity for substrates over that of HIV-1 protease.[9] Similar to the substrate study, in a retrospective study of 128 inhibitors, we observed a high degree of specificity for inhibitors over that of

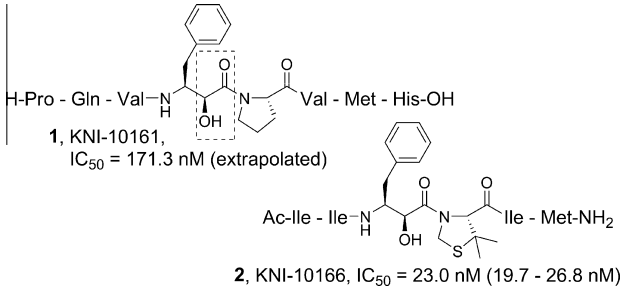

Figure 1. The precursor protein sequence was used to design HTLV-I protease inhibitor **1** that was potency optimized to inhibitor **2**.[16]

* Corresponding author. Tel.: +81 75 595 4635; fax: +81 75 591 9900.
E-mail address: kiso@mb.kyoto-phu.ac.jp (Y. Kiso).

0960-894X/$ - see front matter © 2011 Elsevier Ltd. All rights reserved.
doi:10.1016/j.bmcl.2011.01.048

Table 1
Screening for potent HTLV-I protease inhibition potency in synthesized compounds.

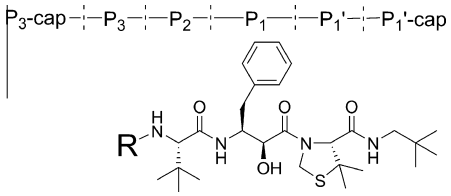

Compounds[17]		R	HTLV-I protease inhibition at 50 nM[16] (%)	HIV-1 protease inhibition at 50 nM[18] (%)
3	KNI-10635	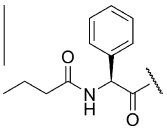	93[a]	99
4	KNI-10680	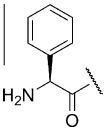	69[a]	>99
5	KNI-10748	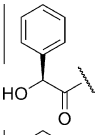	43	92
6	KNI-10747	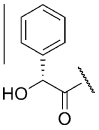	10	82
7	KNI-10777	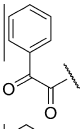	33	76
8	KNI-10751	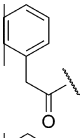	8	22
9	KNI-10750	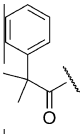	4	80
10	KNI-10765	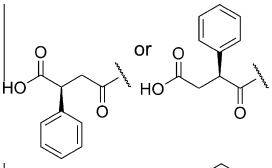	a. 15[b] b. 19	a. 70[b] b. 32
11	KNI-10776	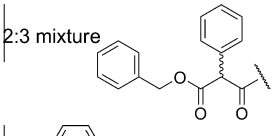	26	34
12	KNI-10755	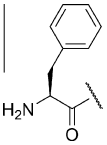	28	>99
13	KNI-10775	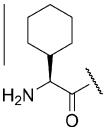	65[a]	99

(*continued on next page*)

Table 1 (*continued*)

Compounds[17]		R	HTLV-I protease inhibition at 50 nM[16] (%)	HIV-1 protease inhibition at 50 nM[18] (%)
14	KNI-10817	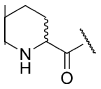	a. 24 b. 11	a. 93 b. 54
15	KNI-10754	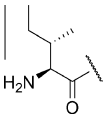	31	97
16	KNI-10842	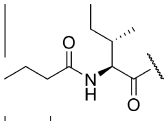	86[a]	95
17	KNI-10814	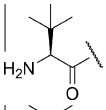	19	95
18	KNI-10813	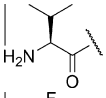	26	96
19	KNI-10774	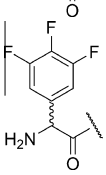	a. 84[a] b. 18	a. >99 b. 68
20	KNI-10843	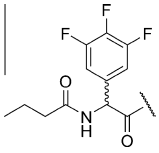	a. 81[a] b. 20	a. >99 b. 80

[a] The IC_{50} values for HTLV-I protease inhibition were determined for compounds **3**, **4**, **13**, **16**, **19a**, and **20a** (Fig. 2).
[b] 1:2 mixture with compound **10b**.

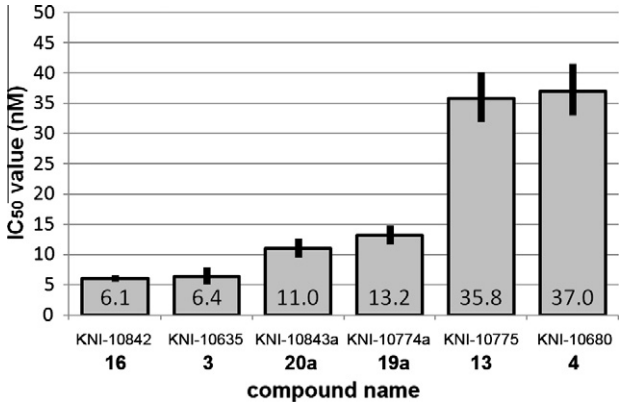

Figure 2. IC_{50} values of potent HTLV-I protease inhibitors.[16]

HIV-1 protease.[19] In other words, HTLV-I protease inhibitors generally also exhibit potent HIV-1 protease inhibition potency, whereas compounds with potent HIV-1 protease inhibition do not necessarily potently inhibit HTLV-I protease. The HTLV-I and HIV-1 protease inhibition profiles in the current study with 18 compounds also support this observation (Table 1). Hence, from a structure-based drug design perspective for HTLV-I protease inhibitors, in our experience, any slight modification in the design of the reference compound tends to drastically affect HTLV-I protease inhibition profile. HIV-1 protease inhibitors, on the other hand, are more forgiving to unfavorable changes. This lack of observed gradation in potency among compounds has made HTLV-I protease inhibitor design much difficult. As a way to overcome this hurdle, in our recent study in which most inhibitors exhibited similarly potent HTLV-I protease inhibition, we used statistical analysis to determine which functional groups were more favored for inhibition, and settled with inhibitor **3**.[15] Along with drug optimization, throughout the years, we also optimized our enzyme assay system to reduce experimental errors.[10,13] About half of the HTLV-I protease expression protein readily autodigests between Leu^{40} and Pro^{41} during isolation and purification.[20] In fact, three out of the seven known cleavage sites in the precursor protein are between a Leu–Pro amide bond, namely matrix–capsid, (transcription factor 1)–protease and protease–p3. Fortunately, autolysis is preventable by a Leu^{40} to Ile^{40} mutation without affecting enzyme kinetics parameters. Our current HTLV-I protease inhibition assay method uses an L40I mutation HTLV-I protease to decrease autoproteolysis, and a fluorescent substrate to increase detection.[21] With our current assay method, we observed that within a narrow range of test inhibitor concentrations between 1 and 100 nM, the percent HTLV-I protease inhibition appreciably changes from none to near complete inhibition. On a side note, another research group reported a chemically synthesized, autocleavage-resistant [Ile^{40}, Ala^{90}, Ala^{109}]HTLV-I protease mutant[22] in which the C90A and C109A mutations improved enzyme stability by preventing intramolecular disulfide bond formation without significantly altering enzyme kinetic properties.[20] According to a recent X-ray crystallography study on several of our tetrapeptidic HTLV-I protease inhibitors in complex with a des-(117–125)-[Ile^{40}]HTLV-I protease[21] and computer-assisted modeling experiments,[15] the oxygen

of the P_3-cap carbonyl function is involved in hydrogen bond interaction with Leu$^{57\prime}$ while the alkyl group of the P_3-cap, as a minor determinant of potency, interacts favorably at the 'entrance' (S_4 subsite) to the active site. Removing the N-terminal P_3-cap moiety from reference inhibitor **3** was shown to decrease inhibition potency against HTLV-I protease, as exemplified by reference inhibitor KNI-10680 (**4**, Table 1).

The goal of the current study is to remove the P_3-cap moiety in our HTLV-I protease inhibitor design. The loss of favorable interactions from the P_3-cap moiety requires compensation by other favorable interactions. General observations from substrate specificity studies on retroviral aspartic proteases[23] along with our study on HTLV-I protease inhibitors[12] suggest that distant subsites from the catalytic S_1–$S_1\prime$ subsites are more tolerant to changes in the substrate or inhibitor. In reference compound **4**, the P_3 residue is farthest from the inhibitor's 'warhead' and is thus relatively more accommodating to modifications. Keeping a phenyl group attached to the alpha carbon atom from the P_3 carbonyl as a pharmacophore, we investigated several modifications (Table 1, **5**–**11**.) The higher potency found in compound **5** over compound **6** supported our X-ray diffraction crystallography data[21] that the *S*-configuration, also found in reference inhibitors **3** and **4**, was better oriented over the *R*-configuration for interactions with the S_3 subsite. Computer-assisted modeling experiments[13–15] and X-ray diffraction crystallography data[21] of related compounds indicate that the amino group in L-phenylglycine in reference inhibitor **4** acts as a hydrogen bond donor to the protease's Asp$^{36\prime}$ side-chain. In consideration that an amino group is a stronger hydrogen bond donor than a hydroxyl group, the relatively weaker inhibition in hydroxyl compound **5** than reference amino compound **4** highlights the importance of this Asp$^{36\prime}$ interaction. A carbonyl group acts as a hydrogen bond acceptor rather than a donor, and thus phenylglyoxylamide **7** which has lower hydrogen bond donating potential than hydroxyl compound **5** predictably exhibited lower inhibition against HTLV-I protease, although bond geometry differences also played a role. In compounds **8** and **9** that cannot form hydrogen bond with Asp$^{36\prime}$, inhibition potency against HTLV-I protease was low. Compounds **10** and **11** were designed to interact with Leu$^{57\prime}$ in a similar way as the P_3-cap carbonyl in reference inhibitor **3**. However, their inhibition against HTLV-I protease was inadequate. The P_3 phenylglycine residue in reference compound **4** was substituted by phenylalanine in compound **12** to observe any change in the reported cation–π interaction between the phenyl group and Arg^{10}'s cationic guanidinyl group,[21] and any appreciative improvement in HTLV-I protease inhibition was not seen. We reconsidered the significance of the cation–π interaction and opted for a cyclohexyl group. Inhibitor **13** (IC_{50} = 36 nM, Fig. 2) with P_3 L-cyclohexylglycine was unexpectedly equipotent to reference inhibitor **4** (IC_{50} = 37 nM). The IC_{50} value was determined for compound **13** and any compound that passed our initial screening assay, that is, compounds with greater than 50% HTLV-I protease inhibition at 50 nM. Believing this to be a breakthrough after so many misses, we examined six-membered ring DL-pipecolic acid (**14**) only to be once again disappointed by a low potency profile. The P_3 L-phenylglycine in reference inhibitors **3** and **4** was initially designed from inhibitor **2** as an isostere of isoleucine (Fig. 1).[13] Although the P_3 isoleucine derivative (**15**) of inhibitor **4** exhibited low potency, the P_3 isoleucine analogue (**16,** IC_{50} = 6 nM) of inhibitor **3** (IC_{50} = 6 nM) was equipotent to its reference. These observations indicate that the P_3-cap *n*-butyramide moiety considerably improves HTLV-I protease inhibition. In the design of reference inhibitors **3** and **4** from compound **2**, L-*tert*-leucine was used as another isostere of isoleucine at the P_2 position. In the current study, the P_3 L-*tert*-leucine derivative (**17**) of reference inhibitor **4** did not present a desirable HTLV-I protease inhibition profile. According to the precursor protein sequence near the protease–p3 cleave site, valine can be accommodated by the S_3 subsite. However, compound **18** with a P_3 valine residue did not exhibit potent HTLV-I protease inhibition. The fluorine atom is often used as a bioisostere of the hydrogen atom that modifies the drug's hydrophilicity profile. In obtaining the X-ray crystallography data of inhibitor–protease complexes in our related compounds, we observed that the more hydrophobic inhibitors were disfavored for co-crystallization with the HTLV-I protease mutant.[21] A perfluorinated analogue with a free amino group may provide an improved hydrophilicity profile. Although the modification was minimal, we were pleasantly surprised that perfluorinated inhibitor **19a** (IC_{50} = 13 nM) was significantly more potent than its reference compound **4**. Extending the N-terminal with an *n*-butyramide capping moiety afforded inhibitor **20a** (IC_{50} = 11 nM) that was slightly more potent or equipotent to free amine inhibitor **19a**, and was somewhat less potent than *n*-butyramide reference inhibitor **3**.

The reactant 3,4,5-trifluorophenylglycine used as the P_3 residue in compounds **19** and **20** is only available commercially as a racemic mixture, and thus the exact configuration for the P_3 residue in the inhibitors, respectively, was not ascertained. However, the HTLV-I protease inhibition profiles of compounds **3**–**6** and **13**, along with the X-ray diffraction crystallography data of closely related compounds[21] strongly suggest that the more potent isolated 'a' fraction in compounds **19** and **20** are likely in an *S*-configuration. Assuming that the P_3 residue is in an *S*-configuration, comparative computer-assisted modeling experiments[24] on inhibitors **3**, **4**, **19a**, and **20a** in complex with a truncated L40I mutation HTLV-I protease were performed using the X-ray crystallography data of similar compounds (PDB IDs: 3LIN and 3LIV).[21] In all inhibitors, hydrogen bond interactions are present throughout the backbone anchoring the docked compound with the catalytic Asp^{32} and Asp$^{32\prime}$ residues from each respective chain of the homodimeric protease, along with Gly$^{34\prime}$, Asp$^{36\prime}$, and Leu$^{57\prime}$ (Fig. 3). Hydrogen bond interactions with Asp^{36} and the flap residues Ala^{59} and Ala$^{59\prime}$ are mediated through water. Hydration of the terminal free amino group in inhibitors **4** and **19a** mediates a link with the amide nitrogen of Leu$^{57\prime}$. This same Leu$^{57\prime}$ amide nitrogen forms a hydrogen bond interaction with the oxygen atom of the P_3-cap in inhibitors **3** and **20a**. The P_3 phenyl group is ideally located and oriented for a non-covalent binding cation–π interaction with Arg^{10}. Overall, the observed hydrogen bond and cation–π interaction patterns are identical in all four compounds (**3**, **4**, **19a**, and **20a**) as well as those found in 3LIN and 3LIV, with differences in Leu$^{57\prime}$ amide nitrogen

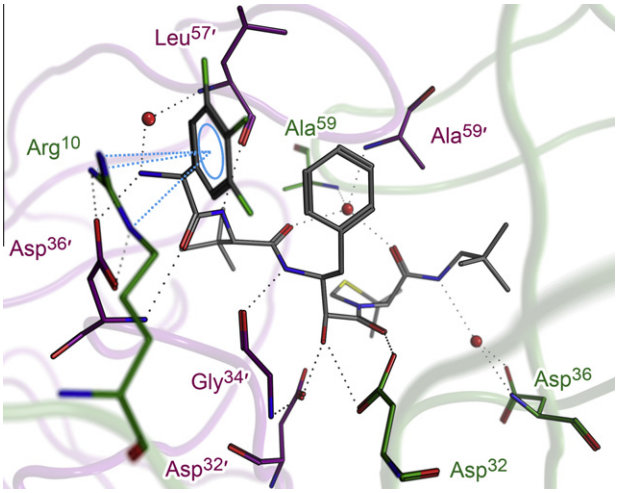

Figure 3. Hydrogen bond (black dotted lines) and cation–π (cyan) interactions in a computer-assisted model of inhibitor **19a** (gray), water (red spheres) and the two chains of HTLV-I protease (purple and green).[24]

interaction, accordingly. The active site of the protease forms a narrow tunnel with hydrogen bond interactions along the inhibitor's backbone perpendicular to subsite interactions (Fig. 4). The inhibitor's P_3 phenyl group is slightly obstructed by Arg^{10} and $Asp^{36\prime}$.

Our previous work demonstrates that the hydrophobic alkyl portion of the P_3-cap moiety is a minor determinant of HTLV-I protease inhibition and thus does not contribute greatly to the inhibition profile.[14,15] The current computer-assisted modeling study indicates that the presence of a P_3-cap moiety in the inhibitor generally greatly increases inhibition against HTLV-I protease due to a direct hydrogen bond interaction between the P_3-cap amide oxygen and $Leu^{57\prime}$ amide nitrogen atoms (Fig. 2). In compounds lacking a P_3-cap moiety, the interaction between the compounds' N-terminal and the $Leu^{57\prime}$ amide nitrogen atom is mediated by a water molecule (Fig. 3). Because water-mediated interactions are weaker than direct hydrogen bond interactions, P_3-capped inhibitors **3**, **16** and **20a** exhibited more potent inhibition potency against HTLV-I protease than free amines **4**, **15**, and **19a**, respectively.

Perfluorination of the P_3 phenyl group affects the cation–π interaction between the aromatic ring and cationic Arg^{10}. Computational studies indicate that electron withdrawing groups weaken the cation–π interaction while electron donating groups strengthen the interaction,[25] via primarily through-space effects of the substituents and secondarily π resonance, instead of being mainly π polarization dependent.[26] Applied to our case, perfluorination of the P_3 phenyl group weakens the cation–π interaction. In the P_3 interaction network, the interaction at the P_3 phenyl group with Arg^{10} indirectly affects the interaction at the P_3 amino group with $Asp^{36\prime}$, because Arg^{10} forms hydrogen bonds with $Asp^{36\prime}$ (Fig. 3).

In free amine compounds, a weak P_3 cation–π interaction may permit sufficient flexibility for the P_3 amino group to finely adjust for a more ideal hydrogen bond interaction with $Asp^{36\prime}$. Consequently, trifluorophenylglycine inhibitor **19a** is more potent than phenylglycine inhibitor **4**, because the hydrogen bond interaction from the P_3 amino group is stronger. Although cyclohexylglycine inhibitor **13** lacks the cation–π interaction, the compound is less potent than trifluorophenyglycine inhibitor **19a**, most likely because compound **13** is bulkier than compound **19a** in regard to hydrophobic interactions at the S_3 subsite, and its bulkiness may also restrict the flexibility of its P_3 amino group. Nevertheless, cyclohexylglycine inhibitor **13** is as potent as reference phenylglycine inhibitor **4**.

In the presence of a P_3-cap moiety, the P_3 amide nitrogen is constrained by the adjacent strong (P_3-cap oxygen)–($Leu^{57\prime}$ nitrogen) hydrogen bond interaction. Consequently, the P_3 amide nitrogen is not as flexible as a free amine nitrogen. As a result, the cation–π interaction contributes additively to the inhibitor–protease interactions, and phenylglycine inhibitor **3** with a P_3-cap moiety is slightly more potent than its perfluorinated derivative (**20a**). The relatively higher potency in isoleucine inhibitor **16** over trifluorophenylglycine inhibitor **20a** may be a result of favored hydrophobic interactions with the S_3 subsite when a P_3-cap moiety is present. In either case, the IC_{50} value range between the comparative P_3-capped inhibitors **3**, **16**, and **20a** is small (6–11 nM) and we may be over-interpreting the inhibition profiles, especially in light that our goal is to discard the P_3-cap moiety.

In summary, the purpose of the current study is to remove the P_3-cap moiety from a very potent tetrapeptidic HTLV-I protease reference inhibitor (**3**, KNI-10635) and to optimize the P_3 phenylglycine moiety for potency by structure-based drug design. Lacking a P_3-cap moiety, the cyclohexylglycine derivative (**13**, KNI-10775) exhibits equipotency to the reference phenylglycine inhibitor (**4**, KNI-10680). To the best of our knowledge, our most potent inhibitor with a 3,4,5-trifluorophenylglycine moiety at the P_3 position (**19a**, KNI-10774a, IC_{50} = 13 nM) represents the smallest and most potent peptidic HTLV-I protease inhibitor in the global scientific community.

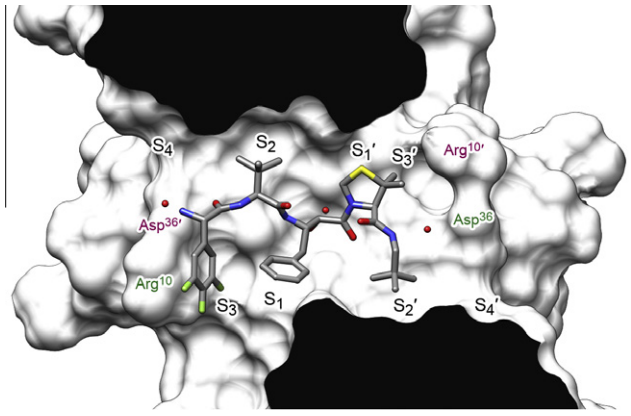

Figure 4. Cross-section top view of computer-assisted model of HTLV-I protease in complex with inhibitor **19a** (black slice plane).[24] Subsite interactions with the inhibitor are perpendicular to hydrogen bond interactions found above ($Leu^{57\prime}$, Ala^{59}, and $Ala^{59\prime}$) and below ($Asp^{36\prime}$, $Gly^{34\prime}$, $Asp^{32\prime}$, Asp^{32}, and Asp^{36}) the plane of the page. See Figure 3 for a side view.

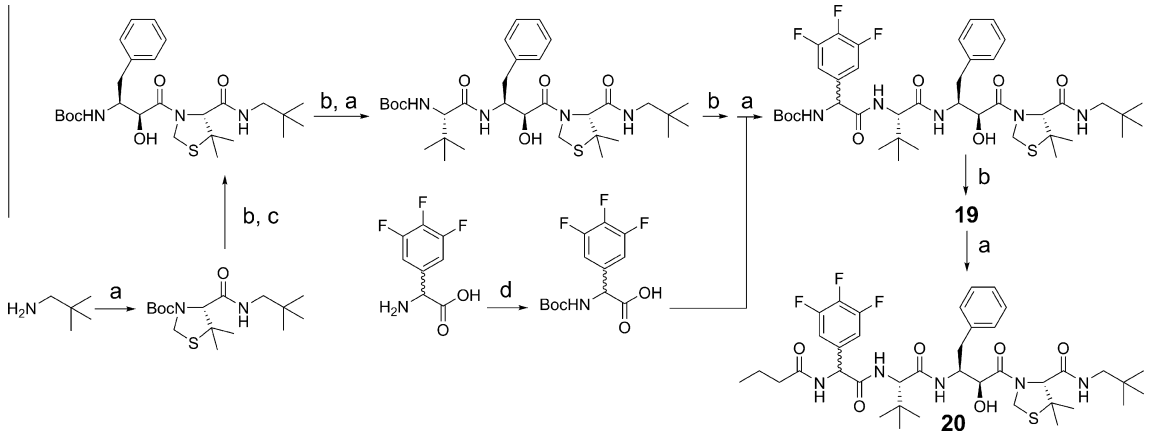

Figure 5. A typical synthetic route for exemplified compounds **19** and **20**.[17] Reaction conditions: (a) 1.2 equiv carboxylic acid, 1.3 equiv BOP, DMF, 1.5 equiv Et_3N, rt overnight, and microwave 50 °C 1 h if low reactivity; (b) 4 N HCl in dioxane, rt 30 min; (c) 1.2 equiv EDC, 1.3 equiv HOBt, DMF, rt 30 min, 1.1 equiv carboxylic acid in DMF gtt, overnight; (d) 1.1 equiv Boc_2O, THF, water, 1.5 equiv Et_3N, rt overnight.

Acknowledgments

This study was supported in part by the 'Academic Frontier' Project for Private Universities, a matching fund subsidy from the Ministry of Education, Culture, Sports, Science and Technology (MEXT), Japan. We thank Mr. T. Hamada for performing HIV-1 protease inhibition assay.

Supplementary data

Supplementary data (IC_{50} plot for compound **19a**; HPLC profiles and MS-data for all target compounds) associated with this article can be found, in the online version, at doi:10.1016/j.bmcl.2011.01.048.

References and notes

1. Nicot, C. *Am. J. Hematol.* **2005**, *78*, 232.
2. Proietti, F. A.; Carneiro-Proietti, A. B.; Catalan-Soares, B. C.; Murphy, E. L. *Oncogene* **2005**, *24*, 6058.
3. Ureta-Vidal, A.; Angelin-Duclos, C.; Tortevoye, P.; Murphy, E.; Lepère, J. F.; Buigues, R. P.; Jolly, N.; Joubert, M.; Carles, G.; Pouliquen, J. F.; de Thé, G.; Moreau, J. P.; Gessain, A. *Int. J. Cancer* **1999**, *82*, 832.
4. Manns, A.; Wilks, R. J.; Murphy, E. L.; Haynes, G.; Figueroa, J. P.; Barnett, M.; Hanchard, B.; Blattner, W. A. *Int. J. Cancer* **1992**, *51*, 886.
5. Nitta, T.; Kanai, M.; Sugihara, E.; Tanaka, M.; Sun, B.; Nagasawa, T.; Sonoda, S.; Saya, H.; Miwa, M. *Cancer Soc.* **2006**, *97*, 836.
6. Takatsuki, K. *Retrovirology* **2005**, *2*, 16.
7. Jacobson, S. *J. Infect. Dis.* **2002**, *186*, 187.
8. Ravandi, F.; Kantarjian, H.; Jones, D.; Dearden, C.; Keating, M.; O'Brien, S. *Cancer* **2005**, *104*, 1808.
9. Kádas, J.; Weber, I. T.; Bagossi, P.; Miklóssy, G.; Boross, P.; Orozslan, S.; Tözsér, J. *J. Biol. Chem.* **2004**, *279*, 27148.
10. Maegawa, H.; Kimura, T.; Arii, Y.; Matsui, Y.; Kasai, S.; Hayashi, Y.; Kiso, Y. *Bioorg. Med. Chem. Lett.* **2004**, *14*, 5925.
11. Bagossi, P.; Kádas, J.; Miklóssy, G.; Boross, P.; Weber, I. T.; Tözsér, J. *J. Virol. Methods* **2004**, *119*, 87.
12. Kimura, T.; Nguyen, J.-T.; Maegawa, H.; Nishiyama, K.; Arii, Y.; Matsui, Y.; Hayshi, Y.; Kiso, Y. *Bioorg. Med. Chem. Lett.* **2007**, *17*, 3276.
13. Nguyen, J.-T.; Zhang, M.; Kumada, H. O.; Itami, A.; Nishiyama, K.; Kimura, T.; Cheng, M.; Hayashi, Y.; Kiso, Y. *Bioorg. Med. Chem. Lett.* **2008**, *18*, 366.
14. Zhang, M.; Nguyen, J.-T.; Kumada, H. O.; Kimura, T.; Cheng, M.; Hayashi, Y.; Kiso, Y. *Bioorg. Med. Chem.* **2008**, *16*, 5795.
15. Zhang, M.; Nguyen, J.-T.; Kumada, H. O.; Kimura, T.; Cheng, M.; Hayashi, Y.; Kiso, Y. *Bioorg. Med. Chem.* **2008**, *16*, 6880.
16. Recombinant L40I mutation HTLV-I protease percent inhibition potency at 50 nM of the test compound was evaluated as single determinations using previously reported procedures.[21] IC_{50} values were calculated from the sigmoid plot derived by percent inhibition data at 1, 5, 10, 20, 50 and 100 nM of the test compound, as single determinations, using Synergy Software's KaleidaGraph (Supplementary data). The error range for IC_{50} values was calculated from the root mean square deviation (RMSD) of the plot, i.e., 50% ± RMSD inhibition.
17. The synthesis of reference compounds **3** and **4** was previously described.[15] Compounds **5**–**20** were synthesized by standard solution phase peptide synthesis by which sequential elongation and coupling of an amine to a carboxylic acid was performed in DMF with benzotriazol-1-yl-oxy-tris-(dimethylamino)phosphonium hexafluorophosphate (BOP) as coupling reagent and Et_3N as base (Fig. 5). Peptide coupling to the P_1 residue was accomplished using 1-ethyl-3-(3-dimethylaminopropyl) carbodiimide hydrochloride (EDC) and 1-hydroxybenzotriazole (HOBt) as additive, without a base, to avoid reported side-reactions.[27] Attachment of a Boc protection group to an amino group was achieved with Boc_2O and Et_3N in THF/water, while the removal of the Boc protection group was achieved with 4 N HCl in dioxane. After preparative HPLC purification, all target compounds (**3**–**20**) were >95% pure by analytical HPLC (Supplementary data). The identities of the compounds were confirmed by TOF MS and ESI-Q MS.
18. Recombinant HIV-1 protease percent inhibition potency at 50 nM of the test compound was evaluated as single determinations using previously reported procedures.[10]
19. Nguyen, J.-T.; Kiso, Y. In Lendeckel, U., Hooper, N. M., Eds.; Viral Proteases and Antiviral Protease Inhibitor Therapy, Proteases in Biology and Disease; Springer Science: Dordretch, 2009; Vol. 8, pp 83–100.
20. Louis, J. M.; Oroszlan, S.; Tözsér, J. *J. Biol. Chem.* **1999**, *274*, 6660.
21. Satoh, T.; Li, M.; Nguyen, J.-T.; Kiso, Y.; Gustchina, A.; Wlodawer, A. *J. Mol. Biol.* **2010**, *401*, 626.
22. Teruya, K.; Kawakami, T.; Akaji, K.; Aimoto, S. *Tetrahedron Lett.* **2002**, *43*, 1487.
23. Tözsér, J.; Zahuczky, G.; Bagossi, P.; Copeland, J. M.; Oroszlan, S.; Harrison, R. W.; Weber, I. T. *Eur. J. Biochem.* **2000**, *267*, 6287.
24. Computer-assisted modeling experiments were performed using Molecular Operating Environment 2009.1001. Visualization of the subsites (Fig. 4) was assisted by UCSF Chimera 1.4.1.
25. Mecozzi, S.; West, A. P., Jr.; Dougherty, D. A. *J. Am. Chem. Soc.* **1996**, *118*, 2307.
26. Wheeler, S. E.; Houk, K. N. *J. Am. Chem. Soc.* **2009**, *131*, 3126.
27. Hayashi, Y.; Kinoshita, Y.; Hidaka, K.; Kiso, A.; Uchibori, H.; Kimura, T.; Kiso, Y. *J. Org. Chem.* **2001**, *66*, 5537.